Impact of urbanisation on formation of urban heat island in Tirupur region using geospatial technique

R Rajkumar*,a & K Elangovanb

aDepartment of Civil Engineering, PSG Institute of Technology and Applied research, Neelambur, Coimbatore – 641 062, India

bDepartment of Civil Engineering, PSG College of Technology, Peelamedu, Coimbatore – 641 004, India

*[E-mail: rajkumar@psgitech.ac.in]

In the recent times, considerable urbanisation has taken place in few places around the world. This urbanisation has occurred due to rapid development in various industries. Furthermore, urbanisation has lead to an increase in movement of the people from rural to urban centres in search of employment. As people kept moving from urban to rural areas there has been a constant demand for the extension of built-up area. As a result of which, the land which was once covered by green vegetation having permeable and low emissivity is now replaced by built-up area with impermeable land and high emissivity. In addition to this, the surface of these built up areas absorbs solar radiation during the day time and emit radiation during the night time and causes increase in surface temperature. The rate of temperature is higher in urban built up area when compared to the rural counterpart making Urban Heat Island (UHI). In this study, an attempt is made to investigate the impact of urbanisation and formation of UHI in the Tirupur region around the corporation limit. The land use land cover (LULC) pattern mapping was carried out through maximum likelihood supervised classification technique for the years 1991, 2001, 2009, 2011 and 2018. Along with this study, Land Surface Temperature (LST) was estimated using Landsat satellite data of the years 2001 and 2018. Furthermore, the impact on LST shows that the urban area has relatively higher LST when compared to the surrounding rural area. Thus it is found that UHI has formed in the region.

[**Keywords**: Urbanisation, Land use land cover, Land Surface Temperature, Urban Heat Island]

Introduction

Urban growth is the key factor for the change in biophysical environment. The unplanned growth in the cities lead to urban sprawl which in turn has significant increase in built up areas and reduction in green covers and barren lands. This urbanisation also leads to movement of people from rural areas to the urban area for their sustainability. The green covers, preamble surfaces and barren lands are replaced by impermeable concrete covers and high emissivity surfaces due to urbanisation. This unplanned growth leads to increase of LST and formation of UHI. LST is raised by the anthropogenic activities such as increase in vehicular movement, energy consumptions, covering the land with materials having high emissivity characteristics etc.[1]. In this study, geospatial techniques have been used to analyse the temperature of the land surface in the study area. In addition, the impact of urban sprawl on the formation of UHI is also studied.

The Landsat series MSS and TM satellite imageries have been used by several researchers to classify the LULC features, as it helps to study the historical land use pattern existing in an area using archived data. The LULC mapping is very important to analyse the changes in urban growth in an area. The LULC changes from 1973 to 1998 were compared with the corresponding LST and Normalized Difference Vegetation Indices (NDVI) from 1987 to 1997. Later the differences were analysed for the Atlanta Metropolitan area using the Landsat series satellite images[2].

The increase in global temperatures affects the sustainability of the cities situated particularly in tropical and sub-tropical regions[3]. Hence, the development in remote sensing technology supports the study of UHI using thermal remote sensing satellite data. The outcome of surface temperature provides a turbulent transfer from the surface and thermodynamic properties such as surface moisture, surface albedo and the near surface effects of atmosphere[4,5]. Many researchers have estimated the LST using Thermal Infrared band of the Landsat series satellite imageries and ASTER satellite thermal images[6] for the geographic locations of Canada[7], Vijayawada city[8] and for Hong Kong city, which are affected by intense UHI[9].

Materials and Methods

Study area

The Tirupur district lies between Latitude 10°14' to 11°20' N, Longitude 77°27' to 77°56' E and cover up an area of 2296 km². The region selected for this study is 1500 Sq. Km. by doing the buffer around corporation limit. It is found that the Western Ghats cover the southern part of the study region, and from West to East the district consists of gradually undulating plain slope. In the first decade of twentieth century, Tirupur was a small panchayat. Later, in 1971, Tirupur became a municipality with 16 councillors comprising of Thennampalayam, Karuvampalayam, and Vallipalayamin south, west and north, respectively. In 2008, by knowing the importance of the town, Tirupur was upgraded to 'Corporation' status by adding nearby town panchayats of Nallur and Vlampalayam and the village panchayats of Thottipalayam, Andipalayam and Mannarai. As per G.O Ms. No. 617, 618 Revenue dated 24.10.2008, the Government of Tamil Nadu formed Tiruppur district by bifurcating four talukas from Coimbatore district (i.e. Tirupur, Udumalpet, Palladam and part of Avinashi) and three taluks from Erode districts (Dharapuram, Kangeyam and part of Perundurai). The illustration of study area is given in Figure 1. Tirupur is an important trade centre of India as far as textile business is concerned. Because of the textile exports, the study region is a major source of foreign exchange due to the city's vital contribution in textile. Moreover, Tirupur plays a major role in the country's growing economy especially during the recent years.
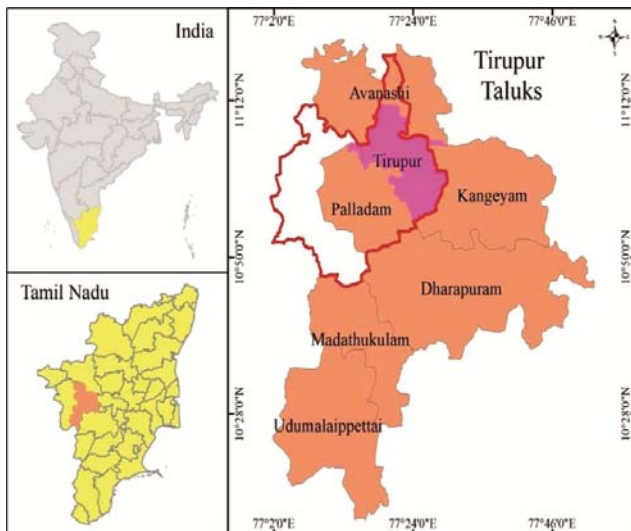
Methodology

In order to predict the UHI in the study region, LULC changes and LST derivation were used. A detailed representation of the methodology used in the present study is given in Figure 2. The LULC analysis gives us the change in land use pattern i.e. increase in built-up area, decrease in barren land and green cover. It is observed that an increase in the temperature and variability in rainfall are the causal factors of the change in pattern in the region.

Land Use Land Cover (LULC) mapping

In the current study, the LULC mapping was carried out using Landsat series multi spectral satellite data (Table 1), downloaded from USGS online portal. The downloaded data for the years 1991, 2001, 2009, 2011, and 2018 was layer stacked to generate the false
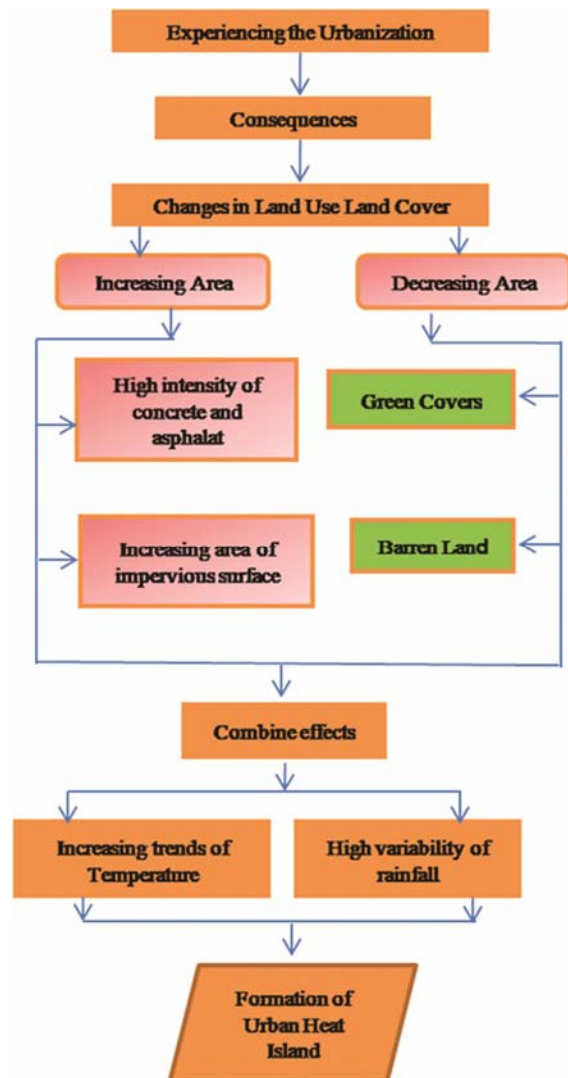

Fig. 1 — Location of the study area – Tirupur town, Tamil Nadu, India

Fig. 2 — Methodology adopted in the present study

Year	Data used	Path/Row	Date of acquisition
1991	Landsat 4-5 TM C1 Level-1	144/052	12th Feb 1991
2001	Landsat 4-5 TM C1 Level-1	144/052	23rd Feb 2001
2009	Landsat 4-5 TM C1 Level-1	144/052	13th Feb 2009
2011	Landsat 4-5 TM C1 Level-1	144/052	03rd Feb 2011
2018	Landsat 8 Level 1	144/052	06th Feb 2018

colour composite (FCC). Along with this study, the LULC mapping was carried out through maximum likelihood supervised classification technique. The LULC classes in the study region were defined with reference to Bhuvan-Indian Geo-Platform of ISRO. Later, the training sets were assigned to each class. Further, land use and land cover classification were carried out for each year.

Estimation of Land Surface Temperature (*LST*)

Land surface temperatures (LST) were estimated using Landsat-5 satellite data for the year 2001 and Landsat-8 satellite data for the year 2018. Thermal-Infrared (TIR) band which is band 6 (10.40 – 12.50 μm) was successfully used for deriving LST[2]. In the case of Landsat-8, LST can be estimated using TIR Band 10 (10.60 – 11.19 μm) and Band 11 (11.50 – 12.51 μm). The following procedure was adopted to derive LST.

Step 1: Conversion to radiance was done using equation 1.

$$L_\lambda = \frac{(LMAX_\lambda - LMIN_\lambda)}{(QCALMAX - QCALMIN)} X (QCAL - QCALMIN) + LMIN_\lambda \dots (1)$$

Where, L_λ = Radiance spectral at the sensor's aperture in W/m^2 * ster * μm); QCAL = the calibrated pixel quantized value in DN; LMIN$_\lambda$ = radiance spectral that is scaled to QCALMIN in W/m^2 * ster * μm; LMAX$_\lambda$ = radiance spectral that is scaled to QCALMIN in W/m^2 * ster * μm; QCALMIN = minimum quantized calibrated pixel value, which corresponds to LMIN$_\lambda$ in DN = 1 for Level 1 Product Generation System products (LPGS); QCALMAX = calibrated pixel quantized maximum value, which corresponds to LMAX$_\lambda$ in DN = 255.

Step 2: Values of radiance were then converted to at-satellite temperatures using equation 2.

$$T(K) = \frac{K2}{ln\left(\frac{K1}{L_\lambda}+1\right)} - 273.15 \qquad \dots (2)$$

Where, T = Effective at-satellite temperature in Kelvin; L_λ = spectral radiance in W/m^2 * ster * μm;

K1 and K2 = calibration constants 607.76 and 1260.56 for Landsat-5 and 774.8853 and 1321.0789 for Landat-8 in W/m^2 * ster * μm, respectively.

The calculated Temperature in Kelvin was converted into degree Celsius by subtracting 273.15.

Step 3: Normalized Difference Vegetation Index (NDVI) was calculated from satellite data using equation 3.

$$NDVI = \frac{NIR - R}{NIR + R} \qquad \dots (3)$$

Where, NIR is Near Infrared Band (Band 4 of Landsat data); R is Infrared Band (Band 3 of Landsat data).

Step 4: Proportion of vegetation (Pv) was calculated using equation 4.

$$P_v = (NDVI - NDVI_{min})/(NDVI_{max} - NDVI_{min})^2 \dots (4)$$

Where, P_V is Proportion of vegetation; NDVI$_{min}$ and NDVI$_{max}$ are minimum and maximum NDVI values calculated using equation 3.

Step 5: Land surface emissivity was calculated using equation 5.

$$e = 0.004 * P_v + 0.986 \qquad \dots (5)$$

Step 6: Finally, LST was calculated using the equation 6.

$$LST = BT/1 + W * \left(\frac{BT}{P}\right) * ln(e) \qquad \dots (6)$$

Where, LST is Temperature of Land Surface; BT = Temperature at satellite calculated using equation 2; W = emitted radiance wavelength (11.5 μm); p = h*c/s (1.438*10^{-2} m K); h = Planck's Constant (6.626 * 10^{-34}Js); s = Boltzmann constant (1.38 * 10^{-23} J/K); c = Velocity of light (2.998 * 10^8 m/s); The calculated p = 14380; 'e' is emissivity calculated using equation 5.

Results and Discussion

The different LULC features classified in the study region include agriculture - crop land, agriculture - plantation, agriculture - Fallow land, built-up land, scrub forest, water bodies, and sandy area. The classified LULC maps for the years 1991, 2001, 2009, 2011, and 2018 are shown in Figure 3. Also, the result of the LULC analysis for the above said years is given in the Table 2. Based on the LULC analysis, increase in built up area and decrease in the green cover over the study region has happened for the past two decades.
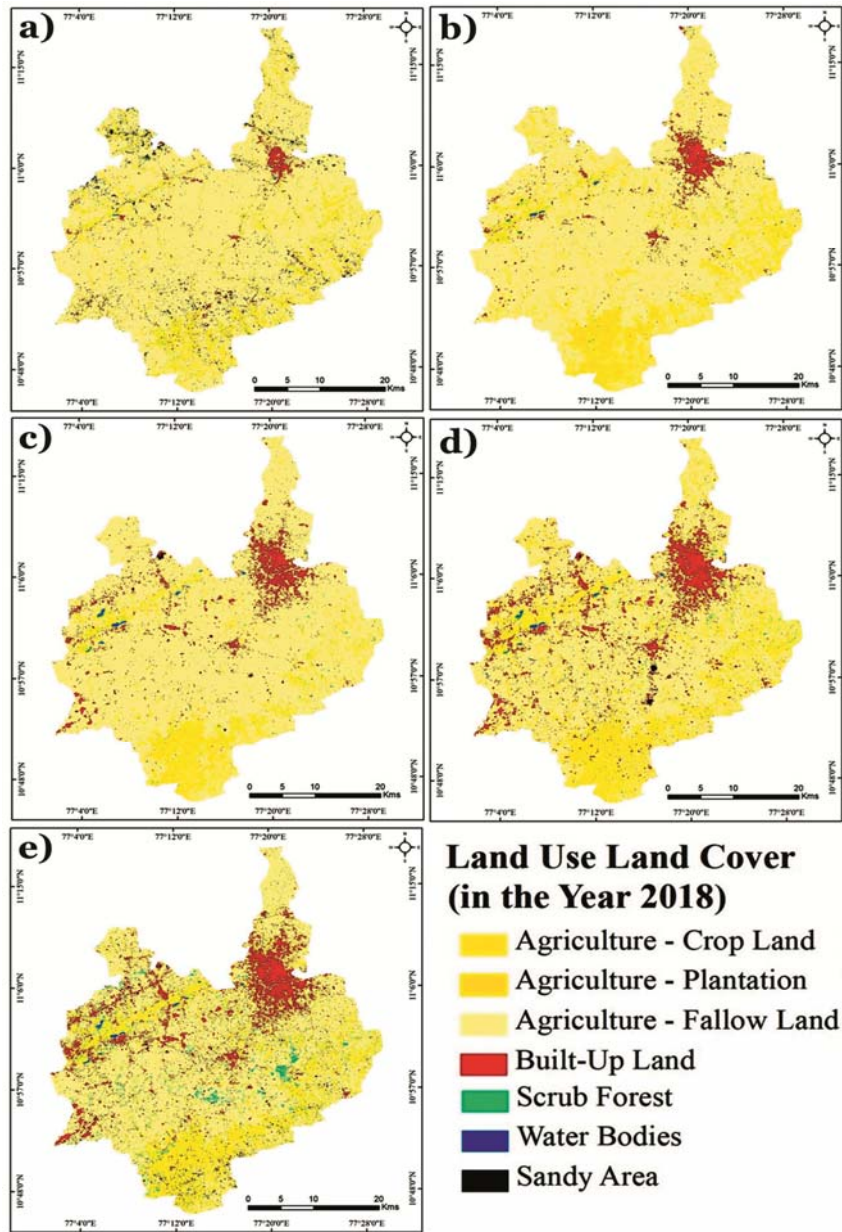
Fig. 3 — Land use land cover: a) 1991; b) 2001; c) 2009; d) 2011; and e) 2018

Table 2 — Classified LULC features and its estimated areal coverage in the study region

LULC Category	Year 1991 (Sq. Km.)	Year 2001 (Sq. Km.)	Year 2009 (Sq. Km.)	Year 2011 (Sq. Km.)	Year 2018 (Sq. Km.)
Agriculture – crop land	187.64	270.48	154.07	353.32	271.35
Agriculture – fallow land	1246.70	1145.19	1246.01	1010.31	1039.39
Agriculture – plantation	9.32	39.11	25.12	8.03	17.67
Built-up land	24.74	41.58	68.43	116.67	119.02
Scrub forest	2.19	1.95	3.42	5.40	27.72
Water bodies	1.30	2.43	2.29	2.55	3.39
Sandy area	31.20	2.37	3.75	6.82	24.56

The built up area in the year 1991 was 24.74 Sq. Km which has drastically changed to 119.02 Sq. Km. The increase in built up area for the study region is shown in Figure 4. This clearly shows the impact of industrialization and high anthropogenic activities in the study region. The difference between increase in the built up area in year 2011 and 2018 is significantly low because of the government policies in the conversion of farm lands for DTCP approval. Also, the decrease in green cover in Tirupur region is shown in Figure 5 from the LULC analysis. It is evident that the anthropogenic heat caused due to human activity such as transportation, manufacturing, heating, cooling and lighting eventually leads to increased UHI.

The built environment for a given urban area deals with urban geometry and dimensions. Furthermore, it is also noted that the heat absorption, shading patterns, the ability of a surface to emit long-wave radiation back to the space and wind movement are influenced by the urban geometry. The urban enclosures such as areas having narrow streets and tall buildings on either side have more effect on UHI. One of the key observations show that the surface temperature is reduced by the tall buildings on daytime by shading the canyons, but the surfaces of those tall buildings may reflect and absorb heat. This results in the increase in the air temperature. The estimated LST values of the year 2001 and 2018 ranges from 22.8121 to 35.6459 and 19.3204 to 31.7428, respectively as shown in Figure 6. The

estimated LST using thermal band of satellite data has been analysed in the month of February for the years 2001 an 2018. The image shows that temperature is very high in the built up area when compared to the rural areas which is covered by green vegetation. It is also found that there is a
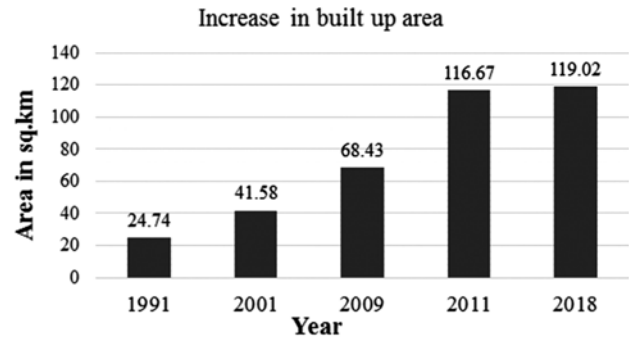

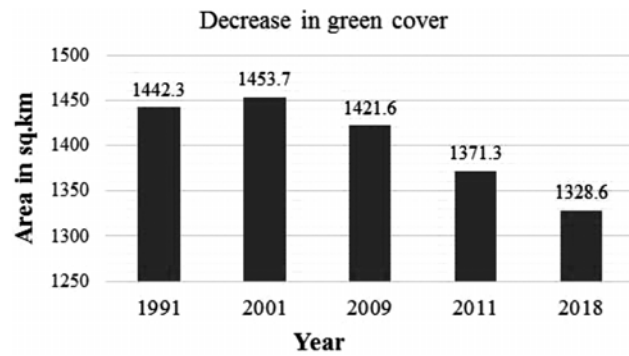Fig. 4 — Increase in Built up area in Tirupur region

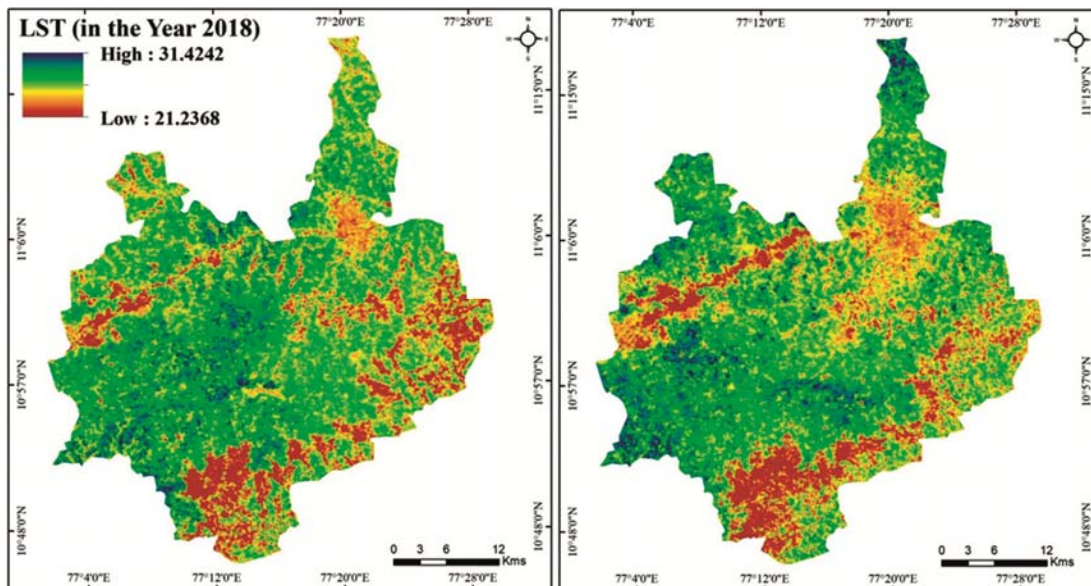Fig. 5 — Decrease in green cover in Tirupur region

Fig. 6 — LST in Tirupur region: a) 2001 and b) 2018

steady rise in land surface temperature from the year 2001 to 2018 in urban area.

Conclusion

Tirupur, is one of the fastest growing cities and also an textile hotspot of the world. In this study, thermal bands in the Landsat-7 satellite were used to extract LST to compare UHI effect with land cover. The results showed that although Tirupur has a moderate temperature, the LST is higher when compared to the rural counterpart. The study clearly indicates the need for green cover and water bodies. Tirupur has undergone the UHI effect due to anthropogenic effects. Hence, this study helps in building an urban environment based on regulation with built geometry, urban built and vegetation. It is recommended that utmost care should be taken by the city planners for ensuring a sustainable development and conversion of green covers to built up area should be avoided.

Acknowledgements

The authors of this paper are grateful to the Management of PSG for extending their support to carry out the research work and granting permission to publish this paper.

Conflict of Interest

The authors declare that there is no conflict of interest.

Author Contributions

Both authors certify that they have participated in the above research work to frame the objective and framework of the study. It includes the participation in the concept, designing the methodology, analysis, writing, or revision of the manuscript. Furthermore, each author certifies that this material or similar material has not been published and will not be submitted or published in any other publication.

References

1 Final Report on Urban Planning Characteristics to Mitigate Climate Change in Context of Urban Heat Island Effect, Bangalore, (The Energy and Resources Institute (TERI)), (2017), pp. 82.

2 Lo C P & Quattrochi D A, Land-Use and Land-Cover Change, Urban Heat Island Phenomenon and Health Implications - A Remote Sensing Approach, *Photo Eng Rem Sens*, 69 (1) (2003) 1053-1063.

3 McCarthy M P, Best M J & Betts R A, Climate change in cities due to global warming and urban effects, *Geophy - Res Letter*, 37 (2) (2010) 1-5.

4 Mirzaei P A & Haghighat F, Approaches to study Urban Heat Island – Abilities and limitations, *Build Environ*, 45 (3) (2010) 2192-2201.

5 Becker F & Li Z L, Surface temperature and emissivity at various scales: Definition, measurement and related problems, *Remote Sens*, 12 (1) (1995) 225-253.

6 Anandababu D & Purushothaman B M, Estimation of Land Surface Temperature using LANDSAT 8 Data, *Int J Adv Res Ideas Innov Technol*, 4 (2018) 177-186.

7 Avdan U & Jovanovska G, Algorithm for Automated Mapping of Land Surface Temperature Using LANDSAT 8 Satellite Data, *J Sensors*, 8 (1) (2016) 1-8.

8 Kumar K S, Bhaskar P U & Padmakumari K, Estimation of Land Surface Temperature to Study Urban Heat Island Effect Using Landsat Etm+ Image, *Int J Engi Sci Tech*, 4 (1) (2012) 772-782.

9 Nichol J E & Hang T P, Temporal characteristics of thermal satellite images for urban heat stress and heat island mapping, *ISPRS J Photogramm Remote Sens*, 74 (3) (2012) 153-162.